

Excitation Spectrum of a Bose-Einstein Condensate

J. Steinhauer, R. Ozeri, N. Katz, and N. Davidson

Department of Physics of Complex Systems, Weizmann Institute of Science, Rehovot 76100, Israel

(Received 3 December 2001; published 12 March 2002)

We report a measurement of the excitation spectrum $\omega(k)$ and the static structure factor $S(k)$ of a Bose-Einstein condensate. The excitation spectrum displays a linear phonon regime, as well as a parabolic single-particle regime. The linear regime provides an upper limit for the superfluid critical velocity, by the Landau criterion. The excitation spectrum agrees well with the Bogoliubov spectrum in the local density approximation, even close to the long-wavelength limit of the region of applicability. Feynman's relation between $\omega(k)$ and $S(k)$ is verified, within an overall constant.

DOI: 10.1103/PhysRevLett.88.120407

PACS numbers: 03.75.Fi, 32.80.Lg, 67.40.Db

The excitation spectrum $\omega(k)$ of superfluid ^4He gives important insights into this superfluid [1]. $\omega(k)$ places an upper bound on the superfluid critical velocity. Furthermore, it indicates the types of excitations which occur in the superfluid, and reflects the superfluid's density correlations. The excitation spectrum of a Bose-Einstein condensate should give similar insight into this system.

The excitation spectrum gives the energy $\hbar\omega(k)$ of each excitation, as a function of its wave vector k . For excitations with wavelengths $2\pi/k$ which are comparable to the radius of the condensate, $\omega(k)$ is characterized by discrete shape-dependent oscillatory modes [2,3]. For wavelengths much shorter than the radius of the condensate in the direction of \vec{k} , $\omega(k)$ becomes an essentially continuous function of k , which characterizes the intrinsic bulk properties of the condensate [4]. In this work, "excitation spectrum" refers to this bulk regime. We report the first measurement of the k dependence of the excitation spectrum.

Previously, isolated points on $\omega(k)$ and their dependence on the chemical potential were measured [5–8].

By definition, $\omega(k)$ is the average frequency of the dynamic structure factor [1] $S(k, \omega)$, which gives the response of the excitation process. Integrating $S(k, \omega)$ over ω gives the static structure factor $S(k)$, which is the Fourier transform of the density correlation function, giving the magnitude of the density fluctuations in the fluid [9], at wavelength $2\pi/k$. In general, the f -sum rule [1] yields Feynman's relation [10]

$$S(k) = (\hbar k^2/2m)/\omega(k). \quad (1)$$

Equation (1) relates the strength of the resonance to its frequency.

For a condensate in a parabolic trap, the density n is inhomogeneous. The condensate can be described by the local density approximation (LDA), as long as the Thomas-Fermi radius of the condensate in the \vec{k} direction is much larger than the wavelength of the excitation [4,6,11]. The zero-temperature $\omega(k)$ in the LDA is

$$\omega(k) = \sqrt{c_{ld}^2(k)k^2 + \left(\frac{\hbar k^2}{2m}\right)^2}, \quad (2)$$

where $c_{ld}(k)$ is given by $\frac{\hbar k}{2m}\sqrt{S(k)^{-2} - 1}$, and [4,6]

$$S(k) = \frac{15}{4} \left\{ \frac{3 + \alpha}{4\alpha^2} - \frac{3 + 2\alpha - \alpha^2}{16\alpha^{5/2}} \right. \\ \left. \times \left[\pi + 2 \arctan\left(\frac{\alpha - 1}{2\sqrt{\alpha}}\right) \right] \right\}, \quad (3)$$

where $\alpha \equiv 2\mu/(\hbar^2 k^2/2m)$ and the chemical potential $\mu = gn(\vec{r} = 0)$, where $n(\vec{r} = 0)$ is the maximum density, g is given by $4\pi\hbar^2 a/m$, and m is the atomic mass. The value $c_{ld}(k)$ is a weak, monotonically increasing function, which varies from $c_{\text{eff}} \equiv 32/(15\pi)\sqrt{\mu/m}$ ($= 0.68\sqrt{\mu/m}$) for small k , to $c_{\text{large}} = \sqrt{4/7}\sqrt{\mu/m}$ ($= 0.76\sqrt{\mu/m}$) for large k . Since $c_{ld}(k)$ is nearly constant, $\omega(k)$ in the LDA (2) is very similar in form to the homogeneous $\omega(k)$ [14] in which $c_{ld}(k)$ is replaced by the constant $c = \sqrt{\mu/m}$, illustrating that $\omega(k)$ of the trapped condensate should largely reflect the intrinsic properties of the homogeneous condensate.

For small k , (2) is given by $\omega(k) \approx c_{\text{eff}}k$, corresponding to phonons with speed c_{eff} . Phonons are collective excitations, each of which consists of a large number [15] N_k of atoms with momentum $\hbar k$, and $N_k - 1$ atoms with momentum $-\hbar k$. This momentum distribution was measured in [8]. Previously, a sound pulse, composed of a combination of phonons, was seen to propagate at roughly c_{eff} [16].

For large k , (2) is given by

$$\omega(k) \approx \hbar k^2/(2m) + mc_{\text{large}}^2/\hbar, \quad (4)$$

where the first term is much larger than the second. This parabolic part of $\omega(k)$ corresponds to single-particle excitations, with velocity much larger than the speed of sound. The second term in (4) is equal to $(4/7)\mu/\hbar$ and is independent of k , reflecting the extra interaction energy [5] experienced by a moving atom [17].

The transition from collective excitations to single-particle excitations occurs for k on the order of ξ^{-1} , where ξ is the healing length [18]. We take ξ^{-1} to be the solution of $k = \sqrt{2}mc_{ld}(k)/\hbar$, which is given by $\xi^{-1} = \sqrt{2}m\bar{c}/\hbar$, and $\bar{c} \approx (c_{\text{eff}} + c_{\text{large}})/2$.

By the Landau criterion, the superfluid critical velocity v_c cannot be greater than ω/k , for any excitation $\omega(k)$ in the spectrum [1]. Note that vortex production usually limits the speed of superfluid flow to a value lower than ω/k [19,20].

Our condensate of ^{87}Rb atoms in the $5s_{1/2}$, $F = 2$, $m_F = 2$ ground state is produced in a QUIC (quadrupole and Ioffe configuration) magnetic trap [21], loaded by a double MOT system. The magnetic trap contains 6×10^7 atoms. After 22 sec of evaporation, 1×10^5 atoms remain, forming a nearly pure condensate, with a thermal fraction of 5% or less. The bias magnetic field is 2 G. The radial and axial trapping frequencies are 220 and 25 Hz, respectively, yielding radial and axial Thomas-Fermi radii of $3 \mu\text{m}$ and $R = 28 \mu\text{m}$, respectively.

$\omega(k)$ is measured by Bragg spectroscopy [5,22]. Two Bragg beams A and B with approximately parallel polarization, separated by an angle $3^\circ \leq \theta \leq 130^\circ$, illuminate the condensate for a time t_B . The frequency of beam A is greater than the frequency of beam B by an amount ω determined by two acousto-optic modulators. If a photon is absorbed from A and emitted into B , an excitation is produced with energy ω and momentum k , where $k = 2k_p \sin(\theta/2)$, and k_p is the photon wave number. Here, we neglect the possibility that a single photon will excite multiple excitations, in contrast to the case of superfluid ^4He [1,23].

The time average of μ/h during the Bragg pulse is determined [24] by the radial size of the condensate after free expansion with and without the pulse, giving $\mu/h = 1.91 \pm 0.09$ kHz, which is taken to be the relevant value for $\omega(k)$.

The wave vector \vec{k} is adjusted to be along the axis of the cigar-shaped condensate. To insure that the entire condensate is stimulated by the Bragg pulse, the length of the pulse t_B is chosen such that the spectral width of the pulse is roughly equal to the intrinsic width of the resonance. For this experiment, the broadening due to inhomogeneous density $\Delta\nu_{ld}$ always dominates the Doppler broadening [5], and is given by [4] 0.45 kHz for large k , and $0.3\omega(k)/(2\pi)$ in the phonon regime. Thus, t_B is chosen to be roughly $(2\Delta\nu_{ld})^{-1}$. For large k , the resonance may be further broadened by s -wave scattering. For $k \geq 6.8 \mu\text{m}^{-1}$, s -wave scattering is clearly visible.

The beams are detuned $\Delta = 6.5$ GHz below the $5S_{1/2}$, $F = 2 \rightarrow 5P_{3/2}$, $F = 3$ transition. The intensities I_A and I_B of each beam are adjusted to values between 0.1 mW cm^{-2} and 1.1 mW cm^{-2} , so that the number of excitations is 10% to 20% of the number of atoms in the condensate. For pulses of this strength, the chemical potential decreases by an average of only 12% during the pulse.

After the Bragg pulse, the atoms are allowed to expand freely, transforming the excitations into free particles [6], which are subsequently imaged by absorption, as shown in Fig. 1. The left and right clouds correspond to the condensate and excitations, respectively.

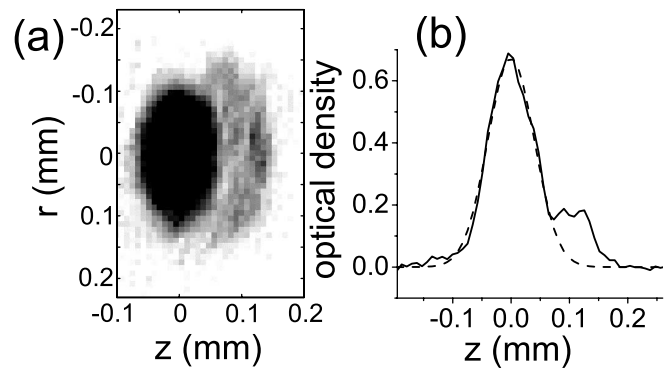


FIG. 1. The Bragg and condensate clouds. (a) Average of two absorption images after 38 msec time of flight, following a resonant Bragg pulse with $k = 2.8 \mu\text{m}^{-1}$, in the phonon regime. (b) Cross section of the same image. The dashed line is a Gaussian fit to the condensate cloud, used to find the zero of momentum. The radial and axial coordinates are indicated by r and z , respectively.

To determine the efficiency of stimulation of excitations by the Bragg pulse, the total momentum in the axial direction relative to the center of the condensate cloud is computed from the image, in the combined regions of the two clouds. The total momentum is divided by $N_o \hbar k$, where N_o is the average number of atoms in the condensate during the Bragg pulse, to obtain the efficiency. This efficiency is somewhat exaggerated though, because the total momentum includes momentum from the release process.

The thus-measured efficiency $P(k, \omega)$ for each direction is shown in Fig. 2, for $k = 2.8 \mu\text{m}^{-1}$. The curve of $P(k, \omega)$ is well approximated by a Gaussian plus a constant. The constant results from the background in the images. The symmetric shape of $P(k, \omega)$ about the resonance frequency probably reflects the spectral shape of the Bragg pulse, rather than the intrinsic shape which is expected to be asymmetric [4]. Therefore, the notation $P(k, \omega)$ is employed, rather than $S(k, \omega)$, whose shape is the intrinsic shape.

The resonant frequency is taken as the center value of the Gaussian fit to $P(k, \omega)$, as shown in Fig. 2. $\omega(k)$ is taken as the average of the resonant frequencies for the left and

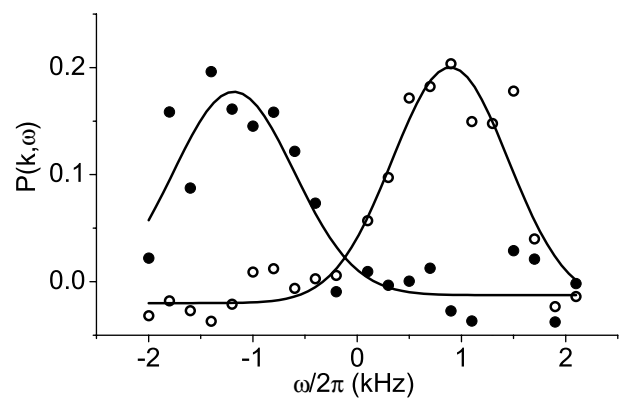


FIG. 2. The efficiency $P(k, \omega)$ for $k = 2.8 \mu\text{m}^{-1}$. The open and filled circles are for left- and right-traveling clouds, respectively. The lines are fits of a Gaussian plus a constant.

right directions, which removes the effects of the Doppler shift resulting from any sloshing of the condensate in the trap during the Bragg pulse.

Figure 3a shows the measured excitation spectrum, which agrees well with (2). A linear phonon regime is seen for low k , and a parabolic single-particle regime for high k . The excitations seen to have the smallest value of ω/k are the phonons. Therefore, by the Landau criterion, the superfluid velocity v_c is bounded by ω/k for the phonons.

The inset of Fig. 3a shows the low k region of $\omega(k)$. To extract the initial slope from the data, (2) is fit to the points with k less than $3 \mu\text{m}^{-1}$, with μ taken as a fit parameter. The fit is not shown in the figure. The result gives the speed of sound for the condensate to be $c_{\text{eff}} = 2.0 \pm 0.1 \text{ mm sec}^{-1}$, which is also the measured upper

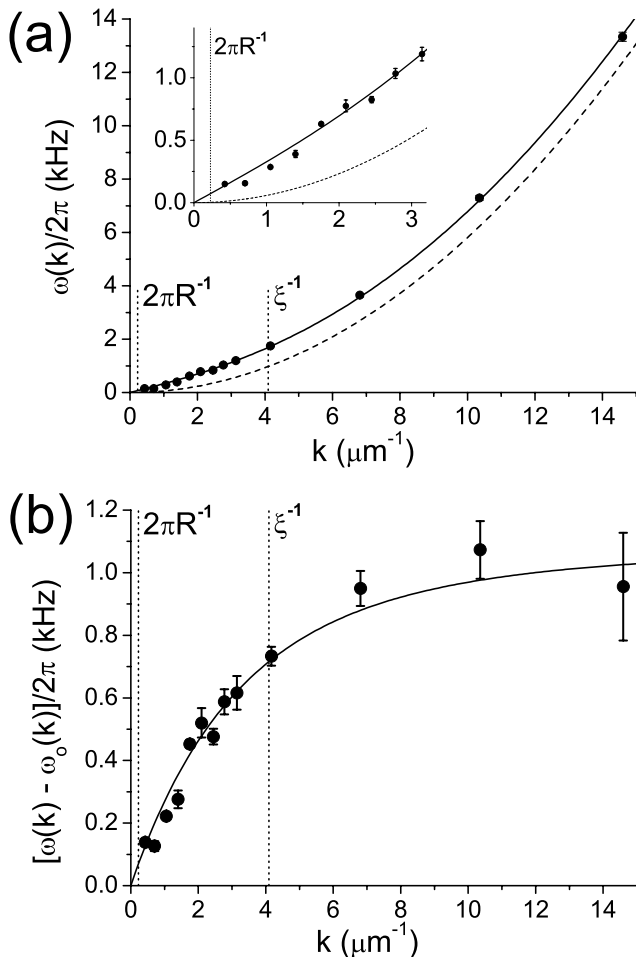


FIG. 3. (a) The measured excitation spectrum $\omega(k)$ of a trapped Bose-Einstein condensate. The solid line is the Bogoliubov spectrum with no free parameters, in the LDA for $\mu = 1.91 \text{ kHz}$. The dashed line is the parabolic free-particle spectrum. For most points, the error bars are not visible on the scale of the figure. The inset shows the linear phonon regime. (b) The difference between the excitation spectrum and the free-particle spectrum. Error bars represent 1σ statistical uncertainty. The theoretical curve is the Bogoliubov spectrum in the LDA for $\mu = 1.91 \text{ kHz}$, minus the free-particle spectrum.

bound for v_c . This value is in good agreement with the theoretical LDA value of $2.01 \pm 0.05 \text{ mm sec}^{-1}$. The line at $2\pi R^{-1}$ indicates the excitation whose wavelength is equal to the Thomas-Fermi radius of the condensate in the axial direction. The measured $\omega(k)$ agrees with the LDA, even for k values approaching this lower limit of the region of validity. As k goes to zero, $\omega(k)$ is seen to approach zero, rather than exciting the lowest order radial mode, the breathing mode, which is twice the radial trapping frequency, 440 Hz [12,13].

In Fig. 3a, the measured $\omega(k)$ is clearly above the parabolic free-particle spectrum $\hbar k^2/(2m)$, reflecting the interaction energy of the condensate. To emphasize the interaction energy, $\omega(k)$ is shown again in Fig. 3b, after subtraction of the free-particle spectrum. This curve approaches a constant for large k , given by the second term in (4).

For a constant rate of production of excitations, the integral of $P(k, \omega)$ over ω , equal to the integral of $S(k, \omega)$, is related to $S(k)$ by [25,26],

$$S(k) = 2(\pi\Omega_R^2 t_B)^{-1} \int P(k, \omega) d\omega, \quad (5)$$

where $\Omega_R = (\Gamma^2/4\Delta)\sqrt{I_A I_B}/I_{\text{sat}}$ is the two-photon Rabi frequency, Γ is the linewidth of the $5P_{3/2}$, $F = 3$ excited state, Δ is the detuning, and I_{sat} is the saturation intensity. The closed circles in Fig. 4 are the measured static structure factor $S(k)$, by (5). The values shown have been increased by a factor of 2.3, giving rough agreement with $S(k)$ from Bogoliubov theory in the LDA (3). Equation (3) is indicated by a solid line. The required factor of 2.3 probably reflects inaccuracies in the various values needed to compute Ω_R . The open circles are computed from (1), using the measured values of $\omega(k)$ shown

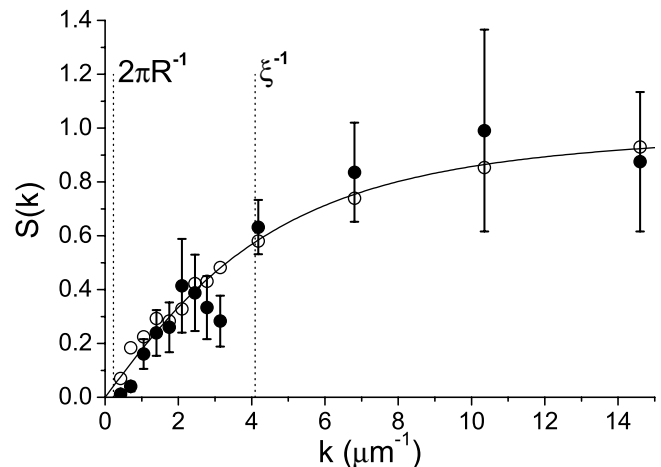


FIG. 4. The filled circles are the measured static structure factor, multiplied by an overall constant of 2.3. Error bars represent 1σ statistical uncertainty, as well as the estimated uncertainty in the two-photon Rabi frequency. The solid line is the Bogoliubov structure factor, in the LDA for $\mu = 1.91 \text{ kHz}$. The open circles are computed from the measured excitation spectrum of Fig. 3, and Feynman's relation (1). For the open circles, the error bars are not visible on the scale of the figure.

in Fig. 3a. The rough agreement between the closed and open circles is consistent with the relation (1), within the multiplicative constant applied to the closed circles. For the determination of $S(k)$, it is critical that the apparent number of excitations is not enhanced by extra momentum obtained during the release process. Therefore, the number of excitations is determined by the number of atoms in the excitation cloud, rather than by the total momentum. This technique fails for the two points with the lowest k values, where many of the atoms do not exit the condensate cloud. For these points, the measured $S(k)$ seen in Fig. 4 is significantly reduced.

For large k (short wavelength), $S(k)$ approaches unity, corresponding to noninteracting, uncorrelated atoms. For long wavelengths, however, $S(k)$ counterintuitively approaches zero. For decreasing k , the condensate contains increasing numbers of atoms with momentum $\hbar k$. These atoms, rather than creating additional density fluctuations with wavelength $2\pi/k$, actually suppress such fluctuations, because the atoms are correlated in pairs with momenta $\pm\hbar k$, and opposite phase [6].

Since $S(k)$ is always less than unity for the values of k measured here, the density fluctuations are never greater than in the uncorrelated case. In contrast, $S(k)$ for superfluid ^4He has a peak (a roton) on the order of $a^3 n$, and a corresponding minimum in $\omega(k)$, at a wavelength comparable to a [1]. In principle, $S(k)$ for the condensate should have a roton at a wavelength comparable to a , which is much shorter than the wavelengths reported here, but for a condensate in an alkali gas, $a^3 n \sim 10^{-4}$, so the roton is negligible.

In conclusion, we report a measurement of the excitation spectrum of a Bose-Einstein condensate, and the static structure factor. The excitation spectrum consists of a linear phonon regime, as well as a single-particle regime. The linear regime provides an upper limit for the superfluid critical velocity, by the Landau criterion. The excitation spectrum agrees quantitatively with the Bogoliubov spectrum, in the local density approximation. The density fluctuations implied by the static structure factor agree with the excitation spectrum within a multiplicative constant, via Feynman's relation. Feynman's relation is thus verified within an overall constant.

We thank F. Dalfovo and M. G. Raizen for helpful comments. This work was supported by the Israel Science Foundation.

[1] Ph. Nozieres and D. Pines, *The Theory of Quantum Liquids* (Addison-Wesley, Reading, MA, 1990), Vol. II.

- [2] D. S. Jin, J. R. Ensher, M. R. Matthews, C. E. Wieman, and E. A. Cornell, *Phys. Rev. Lett.* **77**, 420 (1996).
- [3] M. O. Mewes, M. R. Andrews, N. J. van Druten, D. M. Stamper-Kurn, D. S. Durfee, C. G. Townsend, and W. Ketterle, *Phys. Rev. Lett.* **77**, 988 (1996).
- [4] F. Zambelli, L. Pitaevskii, D. M. Stamper-Kurn, and S. Stringari, *Phys. Rev. A* **61**, 063608 (2000).
- [5] J. Stenger, S. Inouye, A. P. Chikkatur, D. M. Stamper-Kurn, D. E. Pritchard, and W. Ketterle, *Phys. Rev. Lett.* **82**, 4569 (1999).
- [6] D. M. Stamper-Kurn, A. P. Chikkatur, A. Görlitz, S. Inouye, S. Gupta, D. E. Pritchard, and W. Ketterle, *Phys. Rev. Lett.* **83**, 2876 (1999).
- [7] S. Inouye, R. F. Low, S. Gupta, T. Pfau, A. Görlitz, T. L. Gustavson, D. E. Pritchard, and W. Ketterle, *Phys. Rev. Lett.* **85**, 4225 (2000).
- [8] J. M. Vogels, K. Xu, C. Raman, J. R. Abo-Shaer, and W. Ketterle, cond-mat/0109205.
- [9] D. Pines and Ph. Nozieres, *The Theory of Quantum Liquids* (Addison-Wesley, Reading, MA, 1988), Vol. I.
- [10] This relation is derived by other means in R. P. Feynman, *Phys. Rev.* **94**, 262 (1954).
- [11] In [12] and [13], the speed of sound for axial propagation in a cigar-shaped condensate is shown to be approximately the LDA value, even for wavelengths larger than the transverse size of the condensate.
- [12] E. Zaremba, *Phys. Rev. A* **57**, 518 (1998).
- [13] S. Stringari, *Phys. Rev. A* **58**, 2385 (1998).
- [14] N. N. Bogoliubov, *J. Phys. (Moscow)* **11**, 23 (1947).
- [15] A. Brunello, F. Dalfovo, L. Pitaevskii, and S. Stringari, *Phys. Rev. Lett.* **85**, 4422 (2000).
- [16] M. R. Andrews, D. M. Stamper-Kurn, H. J. Miesner, D. S. Durfee, C. G. Townsend, S. Inouye, and W. Ketterle, *Phys. Rev. Lett.* **79**, 553 (1997); *Phys. Rev. Lett.* **80**, 2967(E) (1998).
- [17] A. J. Leggett, *Rev. Mod. Phys.* **73**, 307 (2001).
- [18] G. Baym and C. J. Pethick, *Phys. Rev. Lett.* **76**, 6 (1996).
- [19] C. Raman, M. Kohl, R. Onofrio, D. S. Durfee, C. E. Kuklewicz, Z. Hadzibabic, and W. Ketterle, *Phys. Rev. Lett.* **83**, 2502 (1999).
- [20] R. J. Donnelly, *Quantized Vortices in Helium II* (Cambridge University Press, New York, 1991).
- [21] T. Esslinger, I. Bloch, and T. W. Hänsch, *Phys. Rev. A* **58**, R2664 (1998).
- [22] M. Kozuma, L. Deng, E. W. Hagley, J. Wen, R. Lutwak, K. Helmerson, S. L. Rolston, and W. D. Phillips, *Phys. Rev. Lett.* **82**, 871 (1999).
- [23] A. Griffin, *Excitations in a Bose-Condensed Liquid* (Cambridge University Press, Cambridge, United Kingdom, 1993).
- [24] Y. Castin and R. Dum, *Phys. Rev. Lett.* **77**, 5315 (1996).
- [25] The constant rate of production of excitations is given in W. Ketterle and S. Inouye, e-print cond-mat/0101424 29.
- [26] A. Brunello, F. Dalfovo, L. Pitaevskii, S. Stringari, and F. Zambelli, e-print cond-mat/0104051.